Indian Journal of Chemistry
Vol. 58A, January 2019, pp. 36-44

Effect of mesoporous ruthenium catalysts for hydrogenation of phenol in vapour phase reactor

Jeevanandham Kayalvizhi & Arumugam Pandurangan*

Department of Chemistry, Anna University, Chennai 600 025, Tamilnadu, India

Email: pandurangan_a@yahoo.com/ kayalvizhi.mphil@gmail.com

Received 9 May 2018; revised and accepted 21 December 2018

The catalytic behaviour of RuO_2/SBA-15 has been tested in order to cater to the conversion of phenol to cyclohexanone in a fixed bed reactor. Mesoporous SBA-15 has been synthesized by using hydrothermal method. Different weight percentage (3, 5, 7 wt%) of Ruthenia have been loaded on SBA-15 through wet impregnation method. Physico-chemical characterization of material have been meticulously evaluated by XRD, BET and FT-IR and thermal stability of the catalyst confirmed by TGA analysis. TPR results show the decomposition of RuO_2 to Ru at 300 °C. The oxidation state and chemical composition of the catalyst have been identified by XPS analysis. The morphology of the catalyst has been identified by using SEM and HR-TEM with EDAX techniques. The catalytic activity has been optimized by tweaking different parameter metrics such as temperature, concentration of catalyst, rate of flow of reactant etc., with different iterations. Ruthenium oxide impregnated on carbon and alumina support (activated carbon and Al_2O_3 respectively) has also been examined for hydrogenation reaction and the results compared with that using siliceous support. The maximum conversion of phenol to cyclohexanone has been achieved by passing 4 mL of phenol/h with flow rate of 50 mL of H_2/min (sccm) on 5 wt% at 350 °C using RuO_2/SBA-15 and was confirmed by GC. Lower selectivity of cyclohexanone with decreasing metal loading of RuO_2 on SBA-15 has been observed.

Keywords: Mesoporous RuO_2, SBA-15, Hydrogenation, Phenol, Fixed bed reactors

Hydrogenation of phenol to cyclohexanone is an industrially vital reaction used for the manufacture of nylon 6 and nylon 66, which are significant materials for synthetic fibre and tyre industries[1]. The growth of oil refineries, petrochemical units manufacturing polymeric resins and plastic units have led to the formation of effluents in environmental toxin (phenol)[2]. Huge amounts of phenols and substituted phenols are also obtained by the destruction of primary linkages or C–C linkages of lignin. Normally, the production of cyclohexanone is either by oxidation of cyclohexane or by phenol hydrogenation. The limitation of the oxidation reaction over hydrogenation reaction is due to various factors like temperature, pressure, and recovery of the product[3,4]. So hydrogenation of phenol using supported metal catalyst is a convenient technology to obtain cyclohexanone. Noble metals such as palladium, platinum and ruthenium are multifariously of high cyclohexanone selectivity compared with other metals.

Hydrogenation of phenol using Pt and Pd catalyst was denounced in cyclohexanol and cyclohexanone respectively. Conversion of phenol was enhanced using Pt on alumina and zeolite instead of Pd in vapour phase reactor. This has clearly been depicted by Talukdar *et al*. The order of activation of the molecule on the surface in the hydrogenation of phenol is Pt > Pd > Rh > Ru[5]. Comparative study of catalytic support such as Pd/TiO_2 and Pd/MgO was examined in a microflow reactor by Mahata *et al*. The former is less active when compared to the latter[6]. Eun Jae shin *et al*. studied the preparation of alcoholic solution of phenol with Ni/Y zeolite and Ni/SiO_2 to get cycloalkanes. It shows that on varying time, different products were obtained.

Velu *et al*. explained the same reaction using Pd/meso CeO_2-ZrO_2 and MgO-Al_2O_3. According to them selectivity can be achieved over 1–3wt% Pd loading. Former one produced 50% of cyclohexanone. In the case of MgO, 80% conversion was accomplished at 180 °C. Ce-Fe/SBA-15 displays fascinating diphenol formation on hydroxylation of phenol in the batch reactor. Yanhua Zhang *et al*. apparently observed optimal catalyst for the reaction using a certain amount of Ce/Fe ratio[7]. Yang *et al*. studied the performance on gold and palladium mesoporous spherical hollow spheres as a means of support for hydrogenation of substituted phenol in an autoclave. Selectivity and conversion were enhanced

while adding gold to palladium mesoporous spherical hollow spheres[8]. Diaz *et al*. attempted a study using commercial and homemade Pd supported activated carbon which resulted in high activity and high selectivity towards cyclohexanol [9]. Literature survey reveals that RuO_2/SBA-15 has not been employed so far for hydrogenation reaction, especially in fixed bed reactor. Hydrogenation of phenol using mesoporous supported metal catalyst was given meticulous attention due to their versatile properties like high surface area, large pore volume, tunable pore size and hydrothermal stability[10]. Many researchers introspected that transition metal incorporated on mesoporous materials created active sites. A well-dispersed active center on these porous hosts of mesoporous SBA-15 is always desirable. Due to this reason, only ordered SBA-15 has drawn significant attention, especially as a catalyst [11]. Due to better dispersion, stability of the metals and their electronic transition occur through catalyst making it clear that supportive metals are broadly used[12]. Fortified ruthenium metal oxide acts as an excellent catalyst for hydrogenation reaction[13].

In this work, highly ordered mesoporous SBA-15 was used as a support and different weight percentage of RuO_2 were impregnated on SBA-15. Phenol (reactant) was tested in fixed bed reactor to study the hydrogenation of phenol using Ru/SBA-15. We have explored the activity of the catalyst and optimized the reaction parameters such as temperature, concentration of metal on a support, amount of catalyst and rate of flow of reactant. The effect of different supports such as carbon and alumina for ruthenium loading were also tested for this reaction and the results were compared with those obtained using a siliceous support. The main aim of the study is to convert phenol, as it is a vital lignin-derived compound. It is the first step in the process to convert the lignin (obtained from bio-oil which replaces fossil fuels) to valuable products.

Materials and Methods

Ruthenium (III) chloride trihydrates and tetra ethyl orthosilicate (TEOS) were purchased from Sigma Aldrich and used as the source for ruthenium and silicon respectively. Triblock copolymer poly(ethylene glycol)-block-poly(propylene glycol)-block-poly(ethylene glycol) (Pluronic P_{123}; Mav = 5800, Sigma Aldrich) was used as a surfactant under acidic conditions. Ethanol and Hydrochloric acid were purchased from Merck. Carbon support (activated carbon) and alumina support (aluminum isopropoxide as alumina precursor) were purchased from Sigma Aldrich and Alfa Aesar respectively. All the reagents were used in the reaction without further purification. Phenol was also purchased from Merck.

Preparation of Mesoporous SBA-15

Pure siliceous SBA-15 was synthesized based on the literature reported by Zhao *et al*.[14,15]. In brief, 4 g of Pluronic P_{123} was combined with 120 mL of 2N HCl and 30 mL of 2D water in a polypropylene bottle and stirred at 40 °C until the entire solution was dissolved. To this solution, 8.5 g of tetraethyl orthosilicate (TEOS) was added under vigorous stirring. The contents were stirred for 24 h at 40 °C and later transferred to a Teflon lined autoclave and autoclaved in an oven at 100 °C for 48 h. The above product was filtered and washed with distilled water and ethanol until it turned into a white powder. The powder was collected and calcined at 550 °C for 6 h under air to remove the residual organic template material.

Synthesis of RuO_2-support

A calculated amount ((mol.wt%/At.wt)×0.03)of $RuCl_3.3H_2O$ was impregnated to the 0.97g of SBA-15, using ethanol as solvent (since it was hydrothermally stable) and dried overnight at 100 °C, therafter the product was collected and calcined at 550 °C for 6 h under air to get pure 3 wt% RuO_2/SBA-15. The same procedure was followed to prepare 3, 5, 7 wt% of RuO_2/SBA-15. Similar methods were employed to get Ruthenia impregnated on carbon and alumina support respectively.

Characterization of the catalyst

The XRD pattern was recorded with a PAN Analytical X'Pert diffractometer, using nickel-filtered Cu-Kα radiation (λ = 1.54 Å) using liquid nitrogen-cooled germanium solid-state detector. The diffractogram of XRD was recorded in the 2θ range of 0.5−10° (low angle) and for 10–80° (high angle XRD). The crystalline phase was identified by matching with JCPDS data files.

Nitrogen adsorption-desorption experiments were conducted at −196 °C, with a Quantachrome Quadrasorp gas adsorption analyzer from Micrometrics Instruments. For each and every adsorption measurement, the sample was evacuated at 200 °C at a heating rate 100 °C min^{-1} for 8 h. The surface area was obtained using the Brunauer–Emmett–Teller (BET) model for adsorption with relative pressure ranging from 0.05 to 0.30. The pore volumes were calculated from the amount of N_2 vapours adsorbed at a relative pressure of 0.99. The pore size distribution was evaluated from the desorption branches of the isotherms using the Barrett–Joyner–Halenda (BJH) method.

ICP-AES analysis was performed on Perkin Elmer Optima 5300 DV instruments to determine the chemical composition of the reduced metal catalyst. FT-IR spectra of prepared catalyst were taken on Perkin Elmer (Spectrum RX1) instrument using KBr pellet technique in the range 4000–400 cm^{-1}. Thermogravimetry (TG) studies of used catalysts were carried out under an air flow rate of 30 mL min^{-1} with SDT Q600 V8.0 Build 95 using 2 mg sample and at 0–1000 °C min^{-1} temperature. Hydrogen temperature programmed reduction (H_2-TPR) experiments were measured for the reducibility of the catalyst by employing a Micrometrics Instruments. The catalysts (ca 0.1 g) were placed in a U-shape quartz reactor and equipped with a thermocouple for continuous temperature measurement. Samples were first pretreated at 150 °C by flowing high purity argon to drive away the water or impurities before being cooled down to 50 °C. Then, an Argon gas stream containing 10% H_2 (30 mL min^{-1}) was switched on; the temperature was raised from 50 °C to 800 °C with a rate of 10 °C min^{-1}. The temperature was maintained at 800 °C for 30 min. Hydrogen consumption was monitored using a thermal conductivity detector (TCD).

X-ray photoelectron spectroscopy (XPS) (PHI5000 versa probe II, FEI Inc) was used to identify the elemental compositions and electronic states of the elements.

Scanning electron microscope (SEM) techniques were used to identify the surface morphology of catalyst on a TESCAN VEGA3. High-resolution transmission electron microscopy (HRTEM) is an indispensable tool to check the morphology. The sample was dispersed in ethanol, and ultrasonicated for 30 min, later it was allowed to settle. A drop of the supernatant liquid was then transferred onto a carbon coated copper grid and mounted onto the TEM (JEOL 3010) operated at 300 kV and micrographs were recorded. The presence of elements was identified using energy dispersive X-ray analysis (EDS).

Activity of the catalyst

An accurately weighed quantity of catalyst was packed in the glass reactor which was made up of quartz tube of length 40 cm and internal diameter 2 cm. The catalyst was pre-reduced at ~400 °C temperature for an hour with the help of a tubular furnace controlled by a digital temperature controller. The end of the reactor tube was connected to a coiled condenser and a collector to collect the product. The reactant phenol was kept under saturator for an hour at 70 °C (becomes liquid from crystalline). Phenol was taken in a 30 mL glass syringe and fed into the reactor using syringe infusion pump (Ravel Hiteks, India). The reaction was carried out at atmospheric pressure with 50 mL flow rate of H_2 gas (sccm) by varying temperature, time, concentration and amount of catalyst and later the products were collected. Analysis of the product was carried out by Shimadzu gas chromatograph [model GC-17A RTX-5 fitted with a capillary column (30.0 m×0.25 mm, 0.25 μm film thickness) using flame ionized detector (FID)] with nitrogen as the carrier gas. The recyclability of the catalyst was also verified up to 5 cycles.

% of conversion = (No. of moles of reactant converted)/ (No. of moles of feed)×100

% of selectivity = (No. of moles of particular product produced)/ (Total no. of moles of products produced)×100

Results and Discussion

XRD pattern of the catalyst

The wide-angle XRD of pure siliceous SBA-15 and RuO_2 loaded SBA-15 at a 2θ range of 10–80° is given in Fig. 1. Mesoporous silica shows broad diffraction peaks at a 2θ value of 23° which coincides well with that reported by Sufang Chen *et al*[16]. RuO_2 peaks appear at a 2θ range of 28.1° (110), 35.1° (101), 40.1° (111), 54.3° (211), 58.0° (220), 67.0° (112) and 69.6° (301), according to JCPDS 88–0322 with respective diffraction planes. These results are similar to those inferred by Jung Nam Park *et al*[17]. After the impregnation of RuO_2 on SBA-15, the intensity of diffraction lines appears more, suggesting a fine dispersion of RuO_2 on the SBA-15 material. The *d* spacing and unit cell parameter (a_0) values are determined, and the results are tabulated in Table 1.

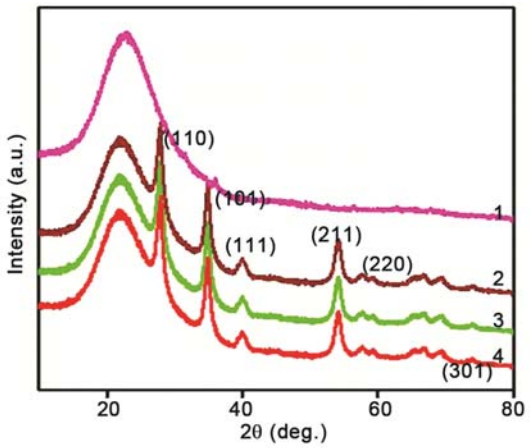

Fig. 1 — High angle XRD of SBA-15 **(1),** 3 wt % RuO_2/SBA-15 **(2)**, 5 wt% RuO_2/SBA-15 **(3)**, and, 7 wt% and RuO_2/SBA-15 **(4)**.

Table 1 — Characterization data of the catalyst

Catalyst	*d* spacing (nm)	Unit cell parameter a_o[a](nm)	BET surface area[b] (m^2/g)	Pore size[b] (nm)	Pore volume[b] (cm^3/g)	Metal content[c] (wt%)
Si-SBA-15	8.8	10.16	612	9.35	1.08	-
3 wt% RuO_2/SBA-15	9.4	10.85	448	9.20	0.81	2.8
5 wt% RuO_2/SBA-15	9.3	10.73	432	9.01	0.77	4.7
7 wt% RuO_2/SBA-15	9.2	10.62	421	9.18	0.74	6.9

[a]Values obtained from XRD analysis. Unit cell parameter was calculated by using the formula $a_o = 2d\ 100/\sqrt{3}$.[b]Values obtained from N2 sorption studies.[c]M content measured by ICP-AES analysis.

The *d* spacing and a_0 value of all the catalysts shows slight marginal differences with the increase in the RuO_2 impregnated on SBA-15, proves the loading of Ruthenia species in the framework of SBA-15 material. It also indicates that the values are dependent on metal loading, which is similar to the results reported by Zhou Jun Wang *et al*[18]. Peaks appearing due to crystalline RuO_2 were observed for Ruthenia catalyst loaded on activated carbon and Al_2O_3 (Fig. 2).

The low angle XRD patterns of mesoporous SBA-15 and RuO_2/SBA-15 are given in Supplementary Data, Fig. S1. It depicts the crystalline nature and *d*-spacing of the materials. The three well-resolved diffraction peaks appear at a 2θ range of 0.9, 1.70 and 1.90 which corresponds to the planes of (100), (110), (200) reflections associated with 2D hexagonal P6*mm* symmetry which has the characteristics of highly ordered mesoporous SBA-15[19]. After impregnation and calcination of different weight percentage of RuO_2 loading, diffraction planes are constant, which proves that there is no significant change in the structure of SBA-15. The decrease in the intensity of XRD peaks is due to the dispersion of Ruthenia within the mesoporous SBA-15[20].

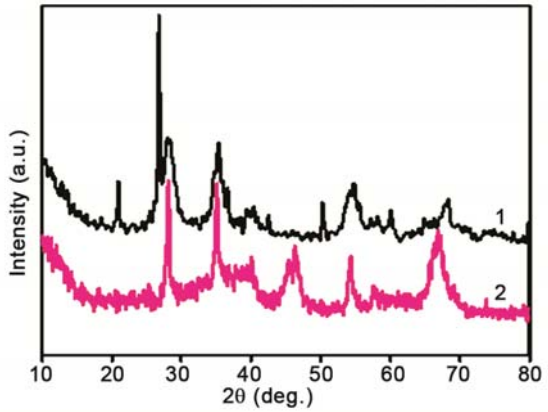

Fig. 2 — High angle XRD of 5 wt% RuO_2/Activated carbon **(1)**, and, 5 wt% RuO_2/Al_2O_3 **(2)**.

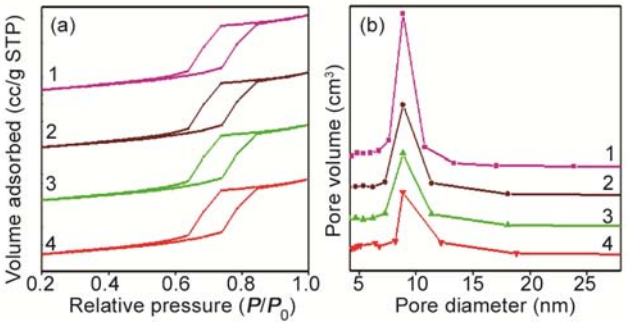

Fig. 3 — (a) N_2 adsorption/desorption isotherm of SBA-15 **(1),** 3 wt% RuO_2/SBA-15 **(2),** 5 wt% RuO_2/SBA-15 **(3)**, and, 7 wt% RuO_2/SBA-15 **(4)**. (b) Pore volume and pore diameter of SBA-15 **(1),** 3 wt% RuO_2/SBA-15 **(2),** 5 wt% RuO_2 SBA-15 **(3)**, and, 7 wt% RuO_2/SBA-15 **(4)** by BJH method.

N_2 adsorption-desorption isotherm

The N_2 adsorption-desorption isotherm and pore size distribution of SBA-15 and RuO_2/SBA-15 are given in Figs 3a & 3b. The isotherm exhibits broad H1 hysteresis loop and capillary condensation of N_2 with uniform mesopores causing sudden steep increase in the relative pressure $P/P_0 = 0.6–0.8$ which corresponds to mesoporous SBA-15 material[21]. BET surface area, pore size and pore volume of mesoporous SBA-15 are found to be 612 $m^2\ g^{-1}$, 9.35 nm, 1.08 $cm^3\ g^{-1}$ respectively, as presented in Table 1. The BET surface area decreases with a function of Ruthenia loading on SBA-15, it might be due to the surface of hydroxyl groups of the SBA-15 consumed by the active phase of the metal precursor[22]. The hysteresis loop declined with increase in RuO_2 loading onto SBA-15. The total pore volume is inversely proportional to Ruthenia loading which happens due to the partial blockage of the Ruthenia clusters. In the case of pore size, the diameter of the Ru/SBA-15 samples have a slightly similar pore size to that of parent SBA-15 with Ru loading. Further increase of Ru content to 7 wt% over SBA-15 results in a decrease of pore size regardless of preparation method of SBA-15 supported RuO catalysts. The pore size distribution of SBA-15 is

narrow and broadening occurs when SBA-15 is loaded with different wt% of RuO. The ICP-AES results of the material are also given in Table 1. It depicts the amount of ruthenium oxide impregnated on the mesoporous SBA-15.

FT-IR analysis

FT-IR spectra of as-synthesised, calcined SBA-15 and RuO_2 loaded SBA-15 catalysts are given in Supplementary Data, Fig. S2. The spectra are recorded from 4000 cm^{-1} to 400 $cm^{-1.}$ A broad band at 3449 cm^{-1} exists in all the spectra, which is due to the -OH stretching vibration of water and defective -OH groups. The characteristic band at 1630 cm^{-1} and 860 cm^{-1} is due to symmetric stretching vibration of Si-OH and Si-O-Si respectively. Peaks at 1200 cm^{-1} and 1080 cm^{-1} belong to symmetric and asymmetric vibration of framework Si-O-Si respectively. Also, 960 cm^{-1} is attributed to Si-O-Si linkages by ruthenium impregnation of silanols. After Ruthenia loading, this band increases with respect to increase in metal loading. A peak at 450 cm^{-1} indicates the presence of bending vibration of the Si-O-Si framework. Similar results are reported with other metal ions loaded on SBA-15[23, 24].

TPR analysis

The most efficient reduction temperature for all the three weight percentages of RuO_2/SBA-15 is at 300 °C and the reduction patterns are displayed in Fig. 4. It is due to the complete reduction of a metallic state of ruthenium from Ru^{3+} to Ru^0. There is no reduction peak at higher temperature. When it reaches 200 °C, ruthenium metal reduces to metallic species and completely reduces at 300 °C. After the reduction of the material, it remains in Ru^0 state[25].

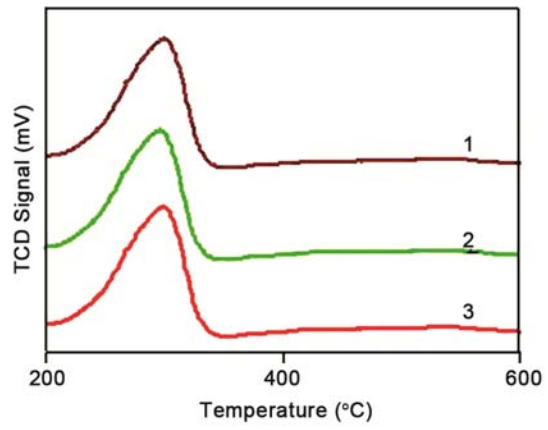

Fig. 4 — TPR Spectrum of 3 wt% RuO_2/SBA-15 **(1)** 5 wt% RuO_2/SBA-15 **(2)**, and, 7 wt% RuO_2/SBA-15 **(3)**.

TGA analysis

Thermogravimetric curves for as-synthesized SBA-15 **(1)**, calcined SBA-15 **(2)** and ruthenium loaded SBA-15 **(3)** material are depicted in Supplementary Data, Fig. S3. For the synthetive compound there is an initial weight loss from 0 °C to 150 °C (3%) which is due to physisorption and chemisorption of water and other weight loss at 150 °C to 400 °C (13%) which is due to the decomposition of template occluded in the pores of SBA-15. There is no weight loss above 400 °C to 800 °C (stable) as shown in Supplementary Data, Fig. S3(1). Calcined SBA-15 and Ruthenia loaded SBA-15 materials are hydrothermally stable upto 800 °C (Supplementary Data, Fig. S3(2) and S3(3)).

XPS analysis

A typical XPS elemental survey scan of 5 wt% RuO_2/SBA-15 is depicted in Fig. 5(a). Ruthenia was detected as minor peaks whereas oxygen and silicon were identified as more intense peaks. The peak between 280 and 290 eV are assigned to Ru $3d^4$ respectively. The peaks present at 104, 155 and 535 eV are attributed to Si2*p*, Si2*s*, and O1*s* respectively. The deconvoluted spectra for Ruthenia are also presented in Fig. 5(b) respectively. The XPS provides the oxidation state and chemical composition of Ru/SBA-15 catalysts. The oxidation state of Ru was identified as a Ru^{2+} 3*d* doublet (5/2 and 3/2) with binding energy values of 280 eV and 284 eV. This suggests the presence of Ruthenia in this material. The intensity of two peaks in the deconvoluted spectra of Ruthenia was found to be low and it shows an uneven distribution of Ruthenia in the material which is in accordance with the HRTEM.

Morphology study of the catalyst

The SEM image of SBA-15 and RuO_2 loaded SBA-15 shows rice like particles with a relatively uniform length of 5 micrometer which is responsible

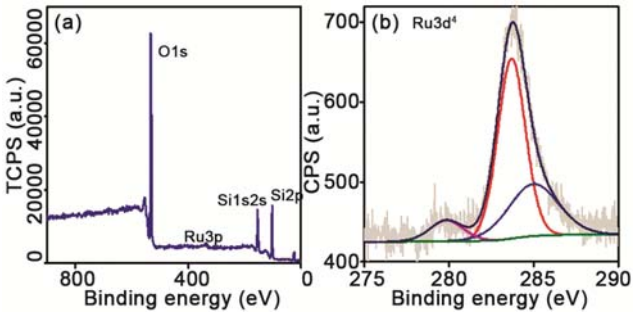

Fig. 5 — XPS spectra of 5 wt% RuO_2/SBA-15 **(1)**, and, deconvluted spectra of Ru **(2)**.

for mesoporous SBA-15. After loading of Ruthenia on SBA-15, porosity was less affected (Supplementary Data, Fig. S4).

The HRTEM images of SBA-15 and Ru loaded SBA-15 shows the presence of highly ordered hexagonal arrays of one-dimensional mesopores, which are characteristic of SBA-15 silica support materials. HRTEM image of mesoporous SBA-15 at two different magnifications are shown in Fig. 6. In addition to impregnating Ruthenia to SBA-15, it could still retain the ordered mesoporous structure as displayed in Fig. 7. HRTEM image of 5 wt% RuO_2/SBA-15 is shown in Fig. 7(a).

The selective area electron diffraction (SAED) pattern (Fig. 7(b)) shows a clear diffraction ring which is indicative of crystallinity of RuO_2 on SBA-15[26]. The dispersion of the Ruthenia particle on the SBA-15 was identified by Image J and presented in Fig. 7 (c). It shows that the Ruthenia particles are unevenly distributed in the SBA-15 matrix. The average particle size was found to be 3.2 nm. The energy dispersive spectrum (EDS) of the material confirms the presence of Si, O_2, and Ru in the RuO_2/SBA-15 (Fig. 7(d)). Un-labelled peak present in the EDS was due to the presence of only oxygen.

Hydrogenation reaction

The hydrogenation of phenol is evaluated by the activity of the RuO_2/SBA-15. About 100 mg of the catalyst is packed in the glass reactor using silica beads and glass wool. The catalyst is pre-reduced at 350 °C with a flow rate of the 50 mL H_2/min (sccm) in each and every run of the reaction. standard cubic centimeter per minute is a unit of mass flow per minute. The various reaction parameters such as reaction temperature, time on stream, amount of catalyst, concentration of the catalyst and catalytic support are studied to get maximum yield of cyclohexanone. Reactant flow was controlled by syringe infusion pump which was denoted by hour whereas gas flow was controlled by mass flow which was denoted by minute.

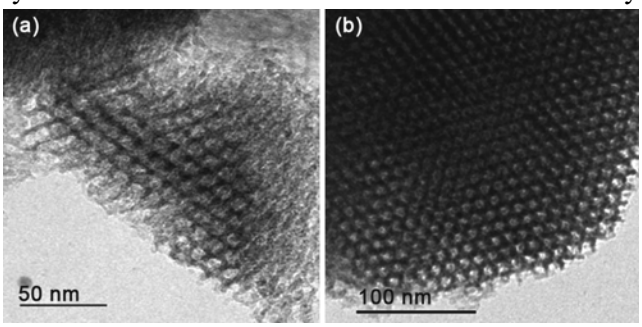

Fig. 6 — HRTEM image of calcined SBA-15 at different magnifications (a) 50 nm, and, (b) 100 nm.

Effect of Temperature

By varying the temperature from 150 °C to 350 °C, temperature study is optimized for about 100 mg of the catalyst. Typically, 4mL of the phenol/h, (rate of flow of H_2) 50 mL/min (sccm) is used to examine the temperature. The effect of temperature (Fig. 8(a)) increases gradually and attains the maximum at 350 °C. It proves that rate of reaction and yield of the product depends on the temperature. The maximum conversion and selectivity of cyclohexanone are higher only at 350 °C as shown in Table 2. Finally, the optimized temperature of the reaction is 350 °C.

Effect of Reactant flow / WHSV

The rate of flow of reactant per weight of the catalyst is termed as weight hour space velocity (WHSV). It exhibits a significant effect on the reaction rate with an increase in the amount of flow of reactant per hour from 4, 8, 12, 16 and 20 mL as shown in Fig. 8(b). The above parameter was studied using about 100 mg of the 5 wt% catalyst at 350 °C, with optimum 50 mL of hydrogen per minute. Conversion of the product is found to be increasing with decrease in the flow of reactant feedstock. Maximum selectivity of cyclohexanone was observed at at 4 mL/h. This proves that much time was required to adsorb the phenol by the Ruthenia metal sites.

Effect of concentration of catalyst

Concentration of the catalyst is defined as the percentage of Ruthenia loaded on the support. To examine different concentrations of the catalyst, 4 mL of the phenol was passed for 350 °C at 50 mL/min (sccm) in 3, 5 and 7 wt% of the catalyst, products were collected separately and the results are given Fig. 8(c). With the increase in Ru loading, the conversion was increasing substantially (3 & 5), but further increase beyond 5 wt% decreased the conversion marginally. It may be due to the increase of ruthenia particle size on the support. Similar results were compared for supported PdO/SBA-15 for the hydrogenation of isophorone[27].

Effect of amount of catalyst

To check the effect of amount of catalyst on the rate, the reaction was carried out by varying the amount of catalyst as 50, 100 and 150 mg, which was packed and pre-reduced separately at 400 °C. The reaction was carried out at an optimized condition of

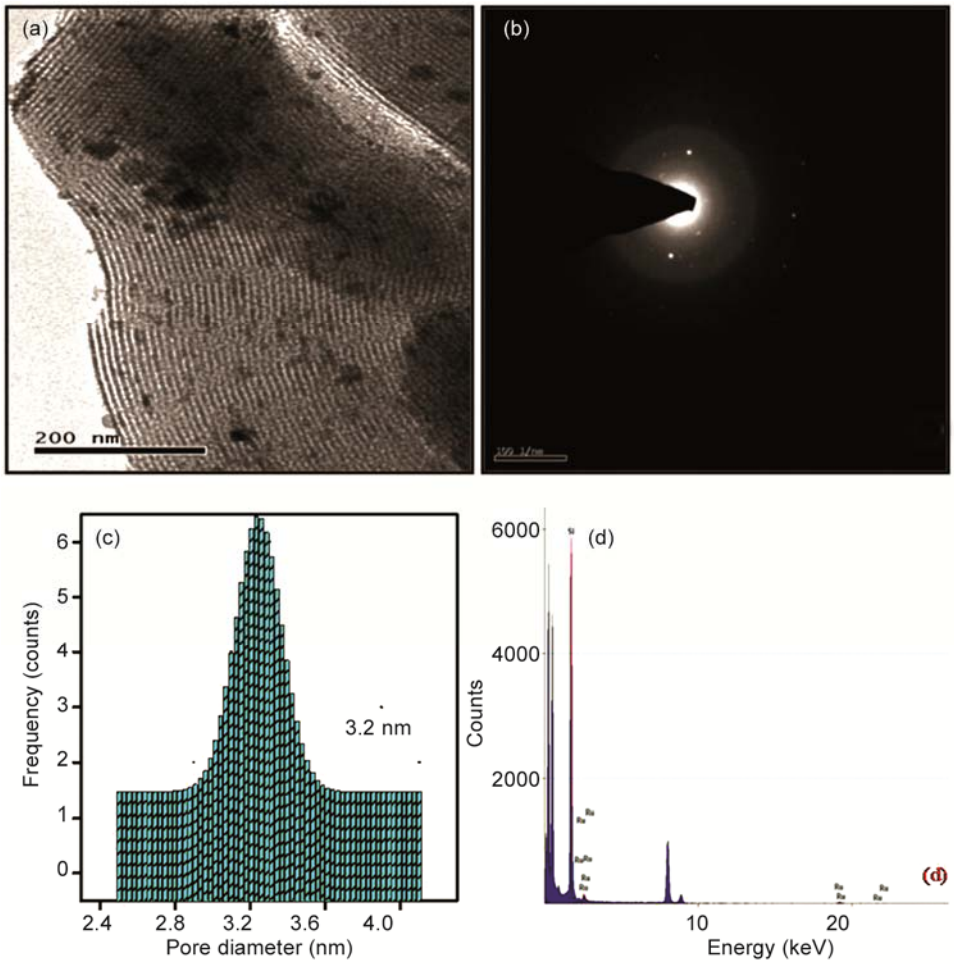

Fig. 7 — HRTEM image of (a) 5 wt% RuO_2/SBA-15, (b) SAED pattern of 5 wt% RuO_2/SBA-15, (c) Particle size distribution of 5 wt% RuO_2/SBA-15, and, (d) EDS of 5 wt% RuO_2/SBA-15.

350 °C with 50 mL of the rate of flow of H_2 (sccm) using 4 mL/h of phenol (Supplementary Data, Fig. S5). It depicts that the amount of catalyst affects the conversion and selectivity of the reaction. The selectivity of cyclohexanone was very high at 100 mg of the catalyst. Amount of catalyst is inversely proportional to the conversion. It may be due to the decrease of active centers and blockage of pores and cages.

Effect of catalytic support and blank

Effect of different catalytic support such as carbon-based support (activated carbon) and alumina support (Al_2O_3) loaded with 5 wt% of ruthenia. At optimized reaction condition, hydrogenation of phenol was carried out and the results are shown in Fig. 8(d). The results show that not much conversion was achieved by using different support at these reaction conditions. No conversion is obtained with non-impregnated ruthenium-free silica (SBA-15) and Fig. 8(d) clearly illustrates that the hydrogenation of phenol occurs effectively using only Ruthenia on mesoporous support. A blank experiment was carried out at the above prescribed reaction condition. The conversion of phenol is 4% and product distribution is surely cyclohexanone.

Recyclability of the catalyst

Recyclability of the catalyst is analyzed to evaluate the activity of the catalyst. The catalyst is utilized repeatedly for around five cycles. By pre-reducing the material at 400 °C at a rate of flow of hydrogen (50 mL /h) for 2 h, the catalyst was recovered. After five cycles, the catalyst is dissolved in ethanol and then calcined at 550 °C. A good reproducibility is achieved by using a recovered catalyst. It reveals the durability and recyclability of the catalyst.

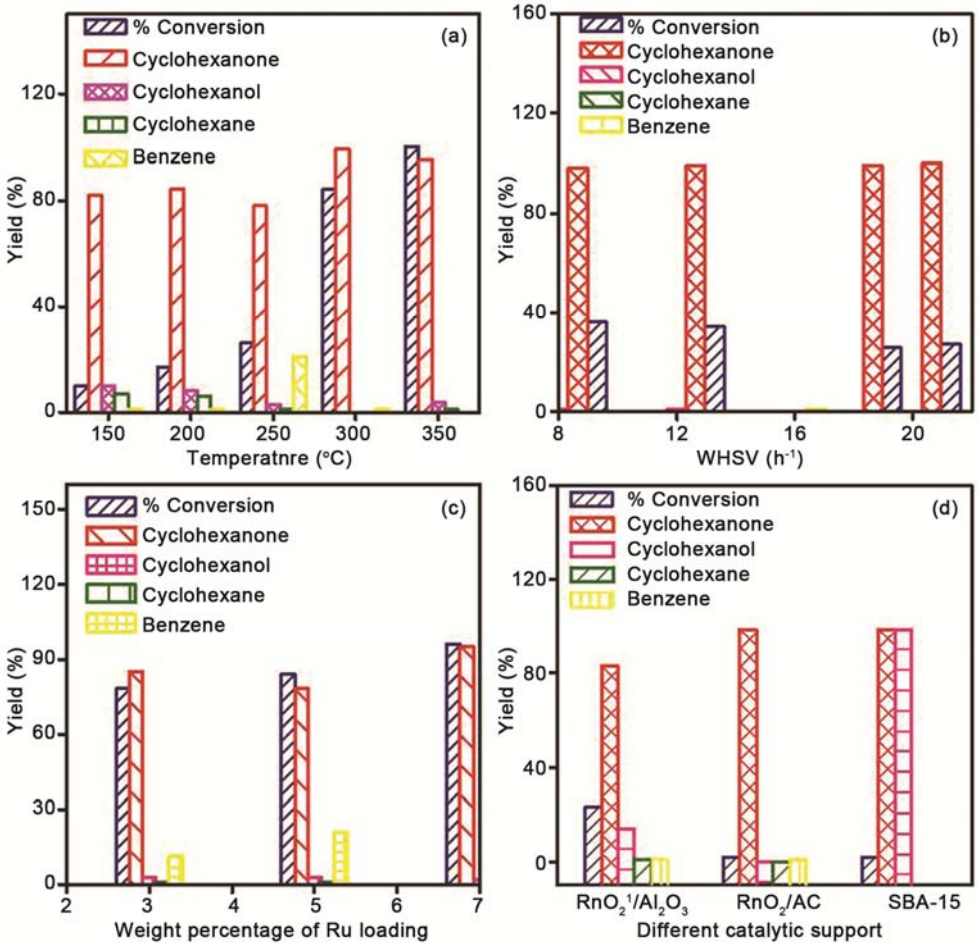

Fig. 8 — (a) Temperature study using 5 wt% RuO_2/SBA-15 (0.1 g) with 50 mL of H_2/minute and 2.0 mL of reactant per hour. (b) WHSV study using 5 wt% RuO_2/SBA-15 (0.1 g) at 300 °C with 50 mL of H_2/minute. (c) Effect of concentration of catalyst studied using RuO_2/SBA-15 with 50 mL of H_2/minute at 300 °C with 4 mL of phenol per hour. (d) Effect of catalytic support studied by varying 5 wt% RuO_2, Activated carbon, Al_2O_3 (0.1 g) with 50 mL of H_2/minute at 300°C with 4 mL of reactant per hour.

Table 2 — Effect of temperature on the hydrogenation of phenol

Temperature (°C)	Conversion (%)	Selectivity (%)			
		Cyclo hexanone	Cyclo hexanol	Cyclo hexane	Benzene
150	10	82	10	7	1
200	17	84	8	6	1
250	26	78	3	1	21
300	84	99	0	0	1
350	100	95	4	1	0

reaction condition: catalyst: 5 wt% RuO_2/SBA-15, duration: 6 h, WHSV: 4 mL/h , H_2 flow: 50 mL/min (sccm).

Conclusions

This work presented the preparation of 5 wt% of RuO_2/SBA-15 catalyst by impregnation method. The XRD pattern of the SBA-15 material displayed 2D hexagonal *P6mm* symmetry with RuO_2 well dispersed on the surface of mesoporous SBA-15. The N_2 adsorption and desorption isotherm confirmed the characteristics of high-quality, mesoporous materials with large pores. The SEM images showed rice like particles of SBA-15, which were not affected by ruthenium loading. HR-TEM images revealed the nature of pore interconnectivity of the large pore of the hexagonal array of siliceous material. The effect of the reaction parameter on the hydrogenation of

phenol using RuO_2/SBA-15 was clearly observed. About 100 mg of the catalyst of 5 wt% RuO_2/SBA-15 with a 50 mL flow rate of hydrogen per min with 4 mL of reactant per hour were optimized to achieve 100 % conversion of cyclohexanone. Hence, from this study, ruthenium dioxide supported SBA-15 is found to be a real catalyst for hydrogenation reaction. Ruthenium-based catalyst showed no sign of deactivation for more than 5 cycles. In view of this, higher lignin-derived model compounds shall be tested for this reaction for the same catalyst in future and their applications in biorefinery production explored.

Supplementary Data

Supplementary Data associated with this article are available in the electronic form at http://www.niscair.res.in/jinfo/ijca/IJCA_58A(01)36-44_SupplData.pdf.

Acknowledgement

The authors gratefully acknowledge the UGC-DRS, DST-FIST sponsored lab in the department of Chemistry, Anna University, Tamil Nadu, India for providing instrumentation facilities for characterization. Institute for Catalysis and Petroleum Technology and Department of Chemistry, Anna University Tamil Nadu, India, is also grateful acknowledged by the authors. The authors acknowledge DST-WOS-a Scheme grant number [SR/WOS-A/CS-104/2013(G)], Department of Science & Technology, Technology Bhavan, New Delhi 110 016, India for awarding financial support.

References

1 Talukdar A K, Bhattacharaya K G & Sivasanker S, *Appl Catal A: General*, 96 (1993) 229.
2 Shin E J & Keane M A, *Ind Eng Chem Res*, 39 (2000) 892.
3 Dodgson I, Griffin K, Barberis G, Piganttaro F & Tauszik G, *Chem Ind*, (1989) 830.
4 Velu S, Kapoor M P, Inagaki S & Suzuki K, *Appl Catal A: General*, 245 (2003)317.
5 Levin M F, Salmeron M, Bell A T & Samorjai G A, *J Chem Soc, Faraday Trans* 83 (1988) 2061.
6 Mahata N, Raghavan K V & Vishwanathan V, *Ind J chem*, 39A (2000) 856.
7 Zhang Y, Gao F, Wan H, Wu C, Kong Y, Wu X, Zhao B, Dong L &Chen Y, *Micropor Mesopor Mater*, 113 (2008) 393.
8 Yang X, Du L, Liao S, Li Y & Song H, *Catal Comm*, 17 (2012) 29.
9 Diaz E, Mohedano A F, Calvo L, Gilarranz M A, Casas J A & Rodriguez J J, *Chem Engg J*, 131(2007) 65.
10 Balamurugan J, Senthil Kumar S M, Thangamuthu R & Pandurangan A, *J Mol Catal A*, 372 (2013) 13.
11 Lin Y C, Li C L, Wan H P, Lee H T, Fang C & Liu, *Energ Fuels*, 25 (2011) 896.
12 Diaz E, Mohedano A F, Calvo L, Gilarranz MA, Casas J A & Rodriguez J J, *Chem Engg J*, 13 (2007) 65.
13 Su B F, Lee F Y, Lv L, Liu J, Tian X N & Zhao X S, *Adv Funct Mater*, 17 (2007) 1926.
14 Zhao D, Huo, Q, Feng, J, Chmelka, B F & Stucky G D, *J Am Chem Soc*, 120 (1998) 6024.
15 Zhao D, Feng J, Huo Q, Melosh N, Fredrickson G H, Chmelka B F & Stucky G D, *Science*, 279 (1998) 548.
16 Lihui Z, Jun H, Sonhai X & Honglai Chin L, *Chem Eng J*, 15 (2007) 507.
17 Li Q, Wu Z X, Tu B, Park S S, Ha C & Zhao D Y, *Micr Mes Mater*, 135 (2010) 95.
18 Chen S, Li J, Zhang Y, Zhao Y, Liew K & Hong J, *Catal Sci Technol*, 4 (2014) 1005.
19 Jung Nam Park, *Reac Kinet Mech Cat*, 103 (2011) 99.
20 Wang Zhou Jun, Xie Yong Bing & Liu Chang Jun, *J Phys Chem C*, 112 (2008) 19818.
21 Ghosh B K, Hazra S, Naik B & Ghosh N N, *Powder Technol*, 269 (2015) 371.
22 Chen L, Hu J, Qi Z, Fang Y & Richards R, *Ind Eng Chem Res*, 50 (2011) 13642.
23 Chary Komandur , Chakravartula VR & Srikanth S, *Catal Lett*, 128 (2009) 164.
24 Taguchi A & Schuth F, *Micr Mes Mater*, 77 (2005) 1.
25 Huang S Y, Chang S M & Yeh C T, *J Phys chem*, 110B (2006) 234.
26 Su F, Lee F Y, Lu Lv, Liu J, Tian X N & Zhao X S, *Adv Funct Mater*, 17 (2007) 1926.
27 Vakati V, Ganji S, Marella R, Seetha Rama Rao K & Burri D R, *Ind J Chem*, 53 (2014) 557.